ARTICLE IN PRESS

Journal of Computational Physics xxx (2009) xxx–xxx

Contents lists available at ScienceDirect

Journal of Computational Physics

journal homepage: www.elsevier.com/locate/jcp

Electromagnetic integral equations requiring small numbers of Krylov-subspace iterations

Oscar Bruno [a,*], Tim Elling [a], Randy Paffenroth [b], Catalin Turc [c]

[a] California Institute of Technology, Applied and Computational Mathematics, MC 217-50, 1200 East California Blvd., CA 91125, United States
[b] Numerica Corporation, 4850 Hahns Peak Drive, Suite 200 Loveland, CO 80538, United States
[c] Case Western Reserve University, Department of Mathematics, 10900 Euclid Ave., Yost Hall 216, Cleveland, OH 44106, United States

ARTICLE INFO

Article history:
Received 21 October 2008
Received in revised form 23 April 2009
Accepted 11 May 2009
Available online xxxx

Keywords:
Electromagnetic scattering
Combined Field Integral Equations
Pseudodifferential operators
Regularizing operator

ABSTRACT

We present a new class of integral equations for the solution of problems of scattering of electromagnetic fields by perfectly conducting bodies. Like the classical Combined Field Integral Equation (CFIE), our formulation results from a representation of the scattered field as a combination of magnetic- and electric-dipole distributions on the surface of the scatterer. In contrast with the classical equations, however, the electric-dipole operator we use contains a regularizing operator; we call the resulting equations Regularized Combined Field Integral Equations (CFIE-R). Unlike the CFIE, the CFIE-R are Fredholm equations which, we show, are uniquely solvable; our selection of coupling parameters, further, yields CFIE-R operators with excellent spectral distributions—with closely clustered eigenvalues—so that small numbers of iterations suffice to solve the corresponding equations by means of Krylov subspace iterative solvers such as GMRES. The regularizing operators are constructed on the basis of the single layer operator, and can thus be incorporated easily within any existing surface integral equation implementation for the solution of the classical CFIE. We present one such methodology: a high-order Nyström approach based on use of partitions of unity and trapezoidal-rule integration. A variety of numerical results demonstrate very significant gains in computational costs that can result from the new formulations, for a given accuracy, over those arising from previous approaches.

1. Introduction

The boundary integral formulations of computational electromagnetics enjoy a number of excellent properties; most notably, they require much smaller discretizations, for a given accuracy, than the three-dimensional discretizations implicit in finite-element or finite-difference approximations of the associated Maxwell equations. Although, in contrast with the differential approaches, integral equations do not give rise to sparse systems of linear equations, the smaller-sized two-dimensional integral-equation discretizations can be exploited through use of fast solvers [5,8,27,30]—which lead to algorithms that can outperform their PDE-approximating counterparts to very significant extents. The computing times required by such fast algorithms, which generally utilize iterative Krylov-subspace-based linear algebra solvers such as GMRES [28], grow linearly, of course, with the numbers of linear algebra Krylov-subspace iterations they require to reach a given error tolerance. In this paper we present a new class of integral equations, *that are of Fredholm type and uniquely solvable for all real wavenumbers*, which evaluate the scattering of electromagnetic waves by perfectly conducting bodies in significantly

* Corresponding author. Tel.: +1 626 395 4548; fax: +1 626 578 0124.
E-mail addresses: bruno@acm.caltech.edu (O. Bruno), lemming@acm.caltech.edu (T. Elling), randy.paffenroth@numerica.us (R. Paffenroth), cct21@case.edu (C. Turc).

0021-9991/$ - see front matter © 2009 Elsevier Inc. All rights reserved.
doi:10.1016/j.jcp.2009.05.020

smaller numbers of Krylov iterations than those required by other formulations. A variety of numerical results demonstrate the very significant gains in computational costs that can result from the new methodology, for a given accuracy, over those arising from previous approaches.

As suggested above, the number of iterations required by an integral-equation iterative solver to reach a given error tolerance depends on the integral equation used. Consider first the classical Magnetic Field Integral Equation (MFIE) and Electric Field Integral Equation (EFIE) for perfectly conducting scatterers [12,21,24], which are uniquely solvable except for an (infinite) discrete set of wavenumbers: the values of the wavenumbers for which the unique solvability is lost coincide with resonant frequencies of the interior Maxwell equations. The existence of such resonances impacts negatively on the numbers of Krylov iterations required by these integral equations for frequencies close to resonance—and, certainly, at resonance both iterative and non-iterative solvers fail to produce the correct, uniquely determined solutions of Maxwell's equations. The best-known approach to address this issue is based on expressing the electromagnetic fields as a superposition of magnetic and electric-dipole distributions, thus combining the MFIE with "$\mathbf{n} \times$ EFIE", see Section 2; the resulting integral equation formulations are referred to as the Combined Field Integral Equations (CFIE) [12,17]. The CFIE is uniquely solvable for every wavenumber, yet, as discussed below, it generally requires large numbers of GMRES iterations for convergence.

(An alternative approach to overcome the difficulties arising from non-uniqueness of MFIE solutions, introduced in [18,32], is based on a concept of dual surfaces. Using an artificial interior surface in addition to the actual scattering surface, the dual MFIE integral penalizes the contribution of the eigenmodes corresponding to the resonant frequencies and renders a uniquely solvable integral equation formulation. According to our experience, however, this equation requires large numbers of iterations—as also does the MFIE even far from resonance; see also comments [22] concerning a certain residual ill conditioning in dual-surface equations.)

As mentioned above, certain characteristics of the uniquely solvable, non-resonant CFIE do influence adversely the iteration counts required by CFIE/GMRES solvers. Indeed, the EFIE operator, which is a portion of the CFIE, is a pseudodifferential operator of order 1—that is, asymptotically, the action of the operator in Fourier space (the highest order asymptotics of which can be uniquely defined by means of local parametrizations and windowed Fourier transforms [29,31]) amounts to multiplication by the Fourier-transform variable. Consistent with this fact, the eigenvalues of these operators accumulate at infinity, which causes CFIE/GMRES algorithms to require large iteration numbers for convergence to a given residual.

A number of approaches have been put forward to remedy the difficulties arising from use of CFIE-based iterative solvers, including, most notably, algebraic preconditioners and analytical regularizers. Algebraic preconditioners, typically involving sparse approximate inverses (see e.g. [10] and references therein), do not exploit the fine structure of the Maxwell equations and the associated integral operators, and, in fact, they do not reduce the numbers of iterations to the extent that might be desirable. Analytical regularizers, in turn, take into account certain subtle properties of the operators underlying the CFIE formulation. An example of such a regularizer is the EFIE operator itself—as it results from the well known Calderón's identities [19], the EFIE operator composed with itself equals the identity plus a compact operator. For smooth closed surfaces this is the actual choice of the regularizer in [2,14,15]; note that the aforementioned EFIE resonances and non-uniqueness are not eliminated by this approach. The approach presented in [15] combines the MFIE with a composition of two EFIE operators for different wavenumbers, one real and one imaginary. Like the CFIE, this coupling appears to overcome the existence of resonant frequencies, although a proof of this fact has not been given as yet. This method was shown to stabilize the number of iterations for simple geometries in the regime of very low frequencies. (Note that the MFIE is itself perfectly suitable in the low frequency regime.) No comments were made in [15] with regards to the behavior of these equations in the more challenging higher-frequency context. Our own experiments in these regards show that, for a given GMRES residual, the latter formulation results in reductions in the numbers of GMRES iterations from those required by the CFIE, but that, still, it requires higher iteration counts than those required by the methods proposed in this text. Considering the fact that, in addition, one matrix–vector product in the overall method [15] is about 1.5 times more expensive than the present counterpart (2.5 times as expensive as the CFIE, while the present approach is only about 1.6 times as expensive as the CFIE), the approach proposed in this text can lead to significantly faster numerics (and, as it happens, higher accuracy for a given discretization) than the approach [15].

A different type of regularizing operators proposed recently [1,3,6] rely on use of approximate high-frequency inverses of the electric field operator; a related approach in the context of acoustic scattering was proposed in [4]. Since the electric field integral operator has different pseudodifferential orders on the spaces of surface gradients and surface rotationals [22], these approaches require decompositions into gradients and rotationals that can be effected at the level of individual elements. Some issues need to be carefully addressed to carry this program to successful completion since, as is known [6], at the discrete level the range of the high-frequency approximations of the admittance operator is not contained within the domain of the electric field integral operator. The approach advocated in [3,6] to remedy this situation calls for use of appropriate projections onto the domain of the electric field operator. These projections can be carried out either via Gram-Schmidt orthogonalizations, which leads to large computational costs [6], or, more efficiently [3], using the numerical fluxes available in the relevant lowest-order finite-element space (known variedly as Raviart–Thomas, RWG and Nédélec edge elements [23,25,26]).

In all, these regularizers provide beneficial effects on iteration numbers, at least in the finite-element context, and for elements of the lowest order. Yet, neither theoretical nor numerical studies of the effect of these projections on the overall error of the solutions have been published—indeed, none of the references [1,3,6,14] contain a quantitative account of the errors resulting from the methodologies proposed for either simple or complex geometries. Efficient generalizations of these ideas

Please cite this article in press as: O. Bruno et al., Electromagnetic integral equations requiring small numbers of Krylov-subspace iterations, J. Comput. Phys. (2009), doi:10.1016/j.jcp.2009.05.020

to higher-order contexts, further, do not seem straightforward. In contrast, the globally defined regularizers introduced in this text are directly amenable to a high-order treatment in the framework of Nyström methods [7]; a variety of numerical results presented in Section 5 attests the high accuracy of the proposed methodology.

The numerical implementation we present of the new regularized equations is a generalization of the Nyström type approach introduced in [7]: we use overlapping partitions of unity and analytical resolution of kernel singularities to evaluate accurately the integral operators. In particular, the extension we present of that approach is capable to treat with high-order accuracy both the hyper-singular integrals involved in the electric integral operator *as well the differential operators involved in the electromagnetic integral equations*. We present numerical results for various test geometries; in all cases our algorithm exhibits high-order convergence.

In view of the reduced additional per-iteration costs inherent in the regularization process we propose, the significant reductions in numbers of iterations they produce, and the high-order accuracies of the corresponding implementations, the new regularized combined field integral equations are highly attractive alternatives to other available formulations, including the classical CFIE as well as improved versions these equations introduced in recent times. An application of the methodologies introduced here to the high-frequency regime requires use of some sort of acceleration technique; an implementation based on a generalization of the equivalent-source acceleration techniques [7] to the new integral equations is underway [9].

This paper is organized as follows: after discussing various classical integral equation formulations in Section 2, in Section 3 we introduce our regularized combined field integral equations. A high-order numerical implementation of these equations is described in Section 4. In Section 5, finally, we present a variety of numerical results produced by these implementations for low-to-medium frequencies.

2. Combined Field Integral Equations

We consider the problem of evaluating the scattered electromagnetic field $(\mathbf{E}^s, \mathbf{H}^s)$ that results as an incident field $(\mathbf{E}^i, \mathbf{H}^i)$ impinges upon the boundary Γ of a perfectly conducting scatterer D. Defining the total field by $(\mathbf{E}, \mathbf{H}) = (\mathbf{E}^s + \mathbf{E}^i, \mathbf{H}^s + \mathbf{H}^i)$, the scattered field is determined uniquely by the Maxwell equations

$$\operatorname{curl} \mathbf{E} - ik\mathbf{H} = 0, \quad \operatorname{curl} \mathbf{H} + ik\mathbf{E} = 0 \quad \text{in } \mathbf{R}^3 \setminus D \tag{1}$$

together with the perfect-conductor boundary conditions

$$n \times \mathbf{E} = 0 \quad \text{on} \quad \Gamma \tag{2}$$

and the radiation condition

$$\lim_{|\mathbf{x}|\to\infty} (\mathbf{H}^s \times \mathbf{x} - |\mathbf{x}|\mathbf{E}^s) = 0, \quad \lim_{|\mathbf{x}|\to\infty} (\mathbf{E}^s \times \mathbf{x} + |\mathbf{x}|\mathbf{H}^s) = 0 \tag{3}$$

uniformly in all directions $\mathbf{x}/|\mathbf{x}|$.

2.1. Direct and indirect EFIE, MFIE and CFIE formulations

A variety of integral equations for this problem exist, including those arising from the *direct method* (which, based on the Stratton–Chu representation formulas [13], express the scattered fields in terms of the physical surface current), as well as those arising from the *indirect method* (that relies on an integral representation based on a non-physical surface density, as discussed in [19]). As is well known, not all possible integral equation formulations for the Maxwell equations are uniquely solvable for all real values of the wavenumbers k: the integral operators underlying some of these equations are not invertible for the values of k that coincide with the eigenvalues of the interior Maxwell problem in D. This is indeed the case for two of the best known such integral equations: the Magnetic Field Integral Equation (MFIE) and the Electric Field Integral Equation (EFIE) [19]; any numerical method based solely on one of these equations will fail to produce a correct approximate solution at and around the resonant frequencies.

The classical approach to overcome this difficulty is based on lumping the MFIE and EFIE formulations into the Combined Field Integral Equation (CFIE), as originally proposed by Harrington and Mautz [17]. As mentioned above, as an alternative to the classical *direct* EFIE, CFIE and MFIE equations just considered, all of which are based on use of the Stratton–Chu formulas, solutions to the Maxwell equations can be sought [12] in terms of corresponding solutions to an *indirect* Combined Field Integral Equation. The direct and indirect combined field equations are uniquely solvable throughout the electromagnetic spectrum, and can thus be utilized as a basis for numerical methods for scattering problems. With the advent of fast algorithms based on iterative linear algebra solvers [28], however, a difficulty inherent in the CFIE formulations became apparent: iterative solvers based on the CFIE require large numbers of iterations; see Section 5.

In detail, the *direct methods* use the Stratton–Chu formulas to express the electric and magnetic fields in terms of the physical current $\mathbf{J} = \mathbf{n} \times \mathbf{H}$ on Γ, leading [24] to the classical MFIE

$$\frac{\mathbf{J}}{2} + \mathcal{K}\mathbf{J} = \mathbf{n} \times \mathbf{H}^i \tag{4}$$

Please cite this article in press as: O. Bruno et al., Electromagnetic integral equations requiring small numbers of Krylov-subspace iterations, J. Comput. Phys. (2009), doi:10.1016/j.jcp.2009.05.020

and EFIE

$$\mathcal{T}\mathbf{J} = -\mathbf{n}\times\mathbf{E}^i. \tag{5}$$

Here the operators $\mathcal{K}$ and $\mathcal{T}$, which map tangential fields $\mathbf{a}$ into tangential fields, are defined by

$$(\mathcal{K}\mathbf{a})(\mathbf{x}) = \mathbf{n}(\mathbf{x})\times\int_\Gamma \nabla_{\mathbf{y}} G_k(\mathbf{x}-\mathbf{y})\times\mathbf{a}(\mathbf{y})d\sigma(\mathbf{y}) \tag{6}$$

and

$$(\mathcal{T}\mathbf{a})(\mathbf{x}) = ik\mathbf{n}(\mathbf{x})\times\int_\Gamma G_k(\mathbf{x}-\mathbf{y})\mathbf{a}(\mathbf{y})d\sigma(\mathbf{y}) + \frac{i}{k}\mathbf{n}(\mathbf{x})\times \mathrm{PV}\int_\Gamma \nabla_{\mathbf{x}} G_k(\mathbf{x}-\mathbf{y})\mathrm{div}_\Gamma\mathbf{a}(\mathbf{y})d\sigma(\mathbf{y}) = (ik\mathbf{n}\times\mathbf{S}_k + \frac{i}{k}\mathcal{T}_{11}\mathrm{div}_\Gamma)\mathbf{a}, \tag{7}$$

where

$$(\mathbf{S}_k\mathbf{a})(\mathbf{x}) = \int_\Gamma G_k(\mathbf{x}-\mathbf{y})\mathbf{a}(\mathbf{y})d\sigma(\mathbf{y}) \tag{8}$$

and

$$(\mathcal{T}_{11}\phi)(\mathbf{x}) = \mathbf{n}(\mathbf{x})\times \mathrm{PV}\int_\Gamma \nabla_{\mathbf{x}} G_k(\mathbf{x}-\mathbf{y})\phi(\mathbf{y})d\sigma(\mathbf{y}) \tag{9}$$

and where G_k is the outgoing fundamental solution of the Helmholtz equation, $G_k(\mathbf{x},\mathbf{y}) = G_k(\mathbf{x}-\mathbf{y}) = \frac{e^{ik|\mathbf{x}-\mathbf{y}|}}{4\pi|\mathbf{x}-\mathbf{y}|}$; the hyper-singular integral in the definition of $\mathcal{K}$ should be interpreted in the sense of Cauchy principal value.

The *indirect methods*, on the other hand, express the scattered electric field in the form of either a magnetic dipole distribution corresponding to a tangential density $\mathbf{m}$

$$\mathbf{E}(\mathbf{x}) = (\mathcal{M}\mathbf{m})(\mathbf{x}) = \mathrm{curl}\int_\Gamma G_k(\mathbf{x}-\mathbf{y})\mathbf{m}(\mathbf{y})d\sigma(\mathbf{y}) \tag{10}$$

or an electric-dipole distribution corresponding to the tangential density $\mathbf{e}$

$$\mathbf{E}(\mathbf{x}) = (\mathcal{E}\mathbf{e})(\mathbf{x}) = \mathrm{curl}\ \mathrm{curl}\int_\Gamma G_k(\mathbf{x}-\mathbf{y})\mathbf{e}(\mathbf{y})d\sigma(\mathbf{y}), \tag{11}$$

while the scattered magnetic field is given by $\mathbf{H}(\mathbf{x}) = \frac{1}{ik}\ \mathrm{curl}\ \mathbf{E}(\mathbf{x})$. Classical continuity properties of vector potentials yield the Indirect Magnetic Field Integral Equation (IMFIE)

$$\frac{\mathbf{m}}{2} - \mathcal{K}\mathbf{m} = \mathbf{n}\times\mathbf{E}^i \tag{12}$$

and the Indirect Electric Field Integral Equation (IEFIE)

$$ik\mathcal{T}\mathbf{e} = \mathbf{n}\times\mathbf{E}^i. \tag{13}$$

The integral equation formulations EFIE (5) and IEFIE (13) differ only by a multiplicative constant and IMFIE (12) and MFIE (4) share the same spurious resonances, as the spectrum of the integral operator $\mathcal{K}$ is symmetric with respect to the origin [19]; thus, from the point of view of iterative solvers the direct and indirect formulations have essentially identical behavior.

The uniquely solvable CFIE [17] is given by a combination of the MFIE and EFIE of the form

$$\frac{\mathbf{J}}{2} + \mathcal{K}\mathbf{J} + \eta_1(\mathbf{n}\times\mathcal{T})(\mathbf{J}) = \mathbf{n}\times\mathbf{H}^i - \eta_1\mathbf{n}\times(\mathbf{n}\times\mathbf{E}^i) \tag{14}$$

with a positive coupling constant η_1. The corresponding Indirect Combined Field Integral Equation (ICFIE), on the other hand, assumes a representation of the type

$$\mathbf{E}(\mathbf{x}) = (\mathcal{M}\mathbf{a} + i\eta_2\mathcal{E}(\mathbf{n}\times\mathbf{a}))(\mathbf{x}) = \mathrm{curl}\int_\Gamma G_k(\mathbf{x}-\mathbf{y})\mathbf{a}(\mathbf{y})d\sigma(\mathbf{y}) + i\eta_2\ \mathrm{curl}\ \mathrm{curl}\int_\Gamma G_k(\mathbf{x}-\mathbf{y})(\mathbf{n}(\mathbf{y})\times\mathbf{a}(\mathbf{y}))d\sigma(\mathbf{y}), \tag{15}$$

$$\mathbf{H}(\mathbf{x}) = \frac{1}{ik}\ \mathrm{curl}\ \mathbf{E}(\mathbf{x}), \quad \mathbf{x}\in\mathbf{R}^3\setminus D, \tag{16}$$

with a positive coupling parameter η_2, where $\mathbf{a}$ is a vector field tangent to Γ. The electromagnetic field just introduced is an outgoing solution to the Maxwell equations with perfectly conducting boundary conditions provided the tangential density $\mathbf{a}$ is a solution to the integral equation

$$\frac{\mathbf{a}}{2} - \mathcal{K}\mathbf{a} + \eta_2 k\mathcal{T}(\mathbf{n}\times\mathbf{a}) = -\mathbf{n}\times\mathbf{E}^i. \tag{17}$$

Standard arguments based on integration by parts show that the integral Eq. (17) is uniquely solvable for all $\eta_2 > 0$ [12].

Please cite this article in press as: O. Bruno et al., Electromagnetic integral equations requiring small numbers of Krylov-subspace iterations, J. Comput. Phys. (2009), doi:10.1016/j.jcp.2009.05.020

3. Regularized Combined Field Integral Equations (CFIE-R)

We introduce regularizing operators $\mathbf{n}\times\mathcal{R}$ in terms of single layer operators with complex wavenumbers which, as demonstrated in Section 5, can lead to significant savings of computing time.

3.1. Generalities

We seek representations of the electromagnetic fields of the form

$$\mathbf{E}^s(\mathbf{x}) = \operatorname{curl}\int_\Gamma G_k(\mathbf{x}-\mathbf{y})\mathbf{a}(\mathbf{y})d\sigma(\mathbf{y}) + i\xi\ \operatorname{curl}\operatorname{curl}\int_\Gamma G_k(\mathbf{x}-\mathbf{y})(\mathbf{n}(\mathbf{y})\times(\mathcal{R}\mathbf{a})(\mathbf{y}))d\sigma(\mathbf{y}), \tag{18}$$

$$\mathbf{H}^s(\mathbf{x}) = \frac{1}{ik}\operatorname{curl}\mathbf{E}(\mathbf{x}), \quad \mathbf{x}\in\mathbf{R}^3\setminus D, \tag{19}$$

where $\mathcal{R}=\mathcal{R}_k$ denotes an operator such that, for any $\xi>0$, $k>0$, the operator $I/2+\xi k\mathcal{T}\circ(\mathbf{n}\times\mathcal{R})$ equals the sum of an invertible operator and a compact operator in the relevant Sobolev spaces of electromagnetic integral equations (see Theorem 3.1 for details); we call $\mathbf{n}\times\mathcal{R}$ a right regularizer for the CFIE. Just as it is the case for the representations considered in Section 2, Eqs. (18) and (19) define outgoing solutions to the Maxwell equations with perfect-conductor boundary conditions provided the tangential density $\mathbf{a}$ is a solution to the integral equation

$$\frac{\mathbf{a}}{2}+\mathcal{K}\mathbf{a}+\xi k\mathcal{T}(\mathbf{n}\times(\mathcal{R}\mathbf{a})) = -\mathbf{n}\times\mathbf{E}^i; \tag{20}$$

this equation will be referred in what follows as the Indirect Regularized Combined Field Integral Equation (ICFIE-R). If $\mathbf{n}\times\mathcal{R}$ is chosen as a right regularizing operator for $\mathcal{T}$, the integral operator on the left-hand side of (20) is a Fredholm operator, and, thus, the unique solvability of Eq. (20) is equivalent to the injectivity of the left-hand side operator.

If, in turn, $\mathbf{n}\times\mathcal{R}$ is a left regularizing operator for $\mathcal{T}$, a *Direct* Regularized Combined Field Integral Equation (DCFIE-R) can be obtained by combining the MFIE (4) with the composition of $\mathbf{n}\times\mathcal{R}$ and the EFIE (5):

$$\frac{\mathbf{J}}{2}-\mathcal{K}\mathbf{J}+\xi k(\mathbf{n}\times\mathcal{R})\circ\mathcal{T}\mathbf{J} = \mathbf{n}\times\mathbf{H}^i-\xi k(\mathbf{n}\times\mathcal{R})(\mathbf{n}\times\mathbf{E}^i). \tag{21}$$

Before considering the actual construction of the operators $\mathcal{R}$, it is useful to note that a classical regularizing operator for $\mathcal{T}$ is provided for smooth closed surfaces by the operator $\mathcal{T}$ itself, as it follows from Calderón projection formulas [11,19]

$$\mathcal{T}^2 = -\frac{\mathbf{I}}{4}+\mathcal{K}^2 \tag{22}$$

together with the fact that the operator $\mathcal{K}$ is compact. This choice of a regularizing operator for $\mathcal{T}$ is at the heart of the efforts in [1,2,14,15]. Although certain simplifications can be taken into account to obtain as efficient numerical evaluations of the operator $\mathcal{T}^2$ as possible (which relate to the fact that the second term in the definition (7) of $\mathcal{T}$ composed with itself yields zero), the work required to evaluate *accurately* the composition $\mathcal{T}^2$ is still comparable to (higher than!) double the work required to evaluate $\mathcal{T}$ once; see Section 5. In our construction, in contrast, the evaluation of the regularizing operator entails an effort comparable to the significantly less expensive evaluation of the first term in the definition (7). Additionally, as mentioned in the introduction, our formulation leads to reduced numbers of iterations.

We use regularizing operators of the form

$$\mathcal{R} = \mathbf{S}_K. \tag{23}$$

for general surfaces Γ.

Remark 3.1. Note that, for certain values of K, the regularizing operator (23) does not make the integral Eq. (20) uniquely solvable—as it can be seen, for a spherical scatterer, using closed-form expressions of the action of the various integral operators on spherical harmonics. As shown in what follows, however, the property of unique solvability is retrieved if the "wavenumber" K is chosen to be purely imaginary—equal to, say, ik_1, and arbitrary constants $k_1\geqslant 0$ and $\xi>0$ are used.

In what follows we denote the regularized indirect operator by

$$\text{ICFIE-R}_K = \frac{I}{2}+\mathcal{K}+\ \xi k\mathcal{T}\circ(\mathbf{n}\times\mathbf{S}_K); \tag{24}$$

for the corresponding direct regularized operator, in turn, we will use the notation

$$\text{DCFIE-R}_K = \frac{I}{2}-\mathcal{K}+\ \xi k(\mathbf{n}\times\mathbf{S}_K)\circ\mathcal{T}. \tag{25}$$

Please cite this article in press as: O. Bruno et al., Electromagnetic integral equations requiring small numbers of Krylov-subspace iterations, J. Comput. Phys. (2009), doi:10.1016/j.jcp.2009.05.020

3.2. Existence and uniqueness

We first establish that, for general closed and smooth manifolds Γ, the composition $\mathcal{T} \circ \mathbf{S}_K$ can be represented as a compact perturbation of an invertible diagonal matrix operator. The main idea in the proof is to use the regularity properties of integral operators with pseudo-homogeneous kernels [29] in the context of the Sobolev spaces $H^{m-\frac{1}{2}}_{\mathrm{div}}(\Gamma)$ of $H^{m-\frac{1}{2}}$ vector fields that admit an $H^{m-\frac{1}{2}}$ divergence [19].

In what follows we use the notations and relations [22,31]:

$$\overrightarrow{\mathrm{curl}}_\Gamma \phi = \nabla_\Gamma \phi \times \mathbf{n}, \tag{26}$$

$$\mathrm{curl}_\Gamma \mathbf{a} = \mathrm{div}_\Gamma(\mathbf{a} \times \mathbf{n}), \tag{27}$$

$$\Delta_\Gamma \phi = \mathrm{div}_\Gamma \nabla_\Gamma \phi = -\mathrm{curl}_\Gamma \overrightarrow{\mathrm{curl}}_\Gamma \phi, \tag{28}$$

where $\mathbf{a}$ is a tangential vector field and where ϕ is a scalar function defined on Γ. A few relevant properties of the Helmholtz decomposition in Sobolev spaces are mentioned in the following Remark.

Remark 3.2. Let Γ be a smooth surface. For a given tangential vector field $\mathbf{a} \in H^{m-1/2}_{\mathrm{div}}(\Gamma)$ we have the Helmholtz decomposition [19,22]

$$\mathbf{a} = \nabla_\Gamma \phi + \overrightarrow{\mathrm{curl}}_\Gamma \psi + \omega, \tag{29}$$

where ω is a harmonic vector field (i.e. its divergence and curl vanish), and where, using the right-inverse [31] $\Delta_\Gamma^{-1} : H^s(\Gamma) \to H^{s+2}(\Gamma)$ of the Laplace-Beltrami operator Δ_Γ, the functions ϕ and ψ in the Helmholtz decomposition (29) are given by $\phi = \Delta_\Gamma^{-1}\ \mathrm{div}_\Gamma\ \mathbf{a}$ and $\psi = -\Delta_\Gamma^{-1} \mathrm{curl}_\Gamma\ \mathbf{a}$. (Note that for simply connected surfaces Γ we necessarily have $\omega = 0$.) Clearly for a tangential vector field $\mathbf{a} \in H^{m-1/2}_{\mathrm{div}}(\Gamma)$ we have $\phi \in H^{m+3/2}(\Gamma)$ and $\psi \in H^{m+1/2}(\Gamma)$ [19]; the corresponding projection operators onto the spaces of gradients, rotationals and harmonic fields will be denoted by

$$\Pi_{\nabla_\Gamma} = \nabla_\Gamma \Delta_\Gamma^{-1}\ \mathrm{div}_\Gamma : H^{m-1/2}_{\mathrm{div}}(\Gamma) \to H^{m+1/2}_{\mathrm{div}}(\Gamma), \tag{30}$$

$$\Pi_{\overrightarrow{\mathrm{curl}}_\Gamma} = \overrightarrow{\mathrm{curl}}_\Gamma \Delta_\Gamma^{-1}\ \mathrm{curl}_\Gamma : H^{m-1/2}_{\mathrm{div}}(\Gamma) \to H^{m-1/2}_{\mathrm{div}}(\Gamma), \text{ and} \tag{31}$$

$$\Pi_{\nabla_\Gamma \cap \overrightarrow{\mathrm{curl}}_\Gamma} = I - \Pi_{\nabla_\Gamma} - \Pi_{\overrightarrow{\mathrm{curl}}_\Gamma} : H^{m-1/2}_{\mathrm{div}}(\Gamma) \to H^{m-1/2}_{\mathrm{div}}(\Gamma). \tag{32}$$

We are now ready to state and prove the main result of this section. Using the notation $A \sim B$ for two operators A and B that differ by a compact operator from $H^{m-\frac{1}{2}}_{\mathrm{div}}(\Gamma)$ to itself, we have

Theorem 3.1. *Let $\mathcal{R} = \mathbf{S}_K$. Then the operator on the left-hand side of* Eq. (20) *satisfies*

$$\frac{I}{2} + \mathcal{K} + \xi k \mathcal{T} \circ (\mathbf{n} \times \mathbf{S}_K) \sim \frac{1}{2}\Pi_{\nabla_\Gamma} + \left(\frac{1}{2} + \frac{i\xi}{4}\right)\Pi_{\overrightarrow{\mathrm{curl}}_\Gamma} + \left(\frac{1}{2} + \frac{i\xi}{4}\right)\Pi_{\nabla_\Gamma \bigcap \overrightarrow{\mathrm{curl}}_\Gamma}. \tag{33}$$

Further, for $K = ik_1, k_1 \geqslant 0,$ and $\xi > 0$, Eq. (20) *admits one and only one solution in the space $H^{m-\frac{1}{2}}_{\mathrm{div}}(\Gamma)$ for any integer $m \geqslant 0$.*

Proof. We first study the electric field integral operator $\mathcal{T}$ defined in Eq. (7). As is well known, denoting by $H^s(TM(\Gamma))$ the classical Sobolev space of tangential vector fields [22], we have [19,22]

$$\mathbf{n} \times \mathbf{S}_k :\ H^s(TM(\Gamma)) \to H^{s+1}(TM(\Gamma)) \tag{34}$$

and thus, in view of either [12, p. 51] or [22]

$$\mathcal{T}_{11} :\ H^s(TM(\Gamma)) \to H^s(TM(\Gamma)). \tag{35}$$

To study the composition $\mathcal{T} \circ (\mathbf{n} \times \mathbf{S}_K)$ we consider the action of this operator on the individual gradient, rotational and harmonic vector fields that make up the Helmholtz decomposition of an arbitrary vector field.

An argument based on integration by parts tells us that the action of the operator $\mathbf{n} \times \mathbf{S}_K$ on gradient fields can be expressed in the form

$$(\mathbf{n} \times \mathbf{S}_K)(\nabla_\Gamma \phi)(\mathbf{y}) = -\overrightarrow{\mathrm{curl}}_\Gamma \int_\Gamma G_K(\mathbf{y} - \mathbf{z})\phi(\mathbf{z}) d\sigma(\mathbf{z}) + \mathbf{n}(\mathbf{y}) \times \int_\Gamma \frac{\partial G_K(\mathbf{y} - \mathbf{z})}{\partial \mathbf{n}(\mathbf{z})} \mathbf{n}(\mathbf{z}) \phi(\mathbf{z}) d\sigma(\mathbf{z}). \tag{36}$$

(To establish (36), integrate by parts the left-hand side of this equation and express the surface gradient of G as a three-dimensional gradient minus the normal derivative times the normal. We thus obtain

$$\mathbf{n}(\mathbf{y}) \times \int_\Gamma \nabla^{\mathbf{y}} G_K(\mathbf{y} - \mathbf{z})\phi(\mathbf{z}) d\sigma(\mathbf{z}) + \int_\Gamma \frac{\partial G_K(\mathbf{y} - \mathbf{z})}{\partial \mathbf{n}(\mathbf{z})} \mathbf{n}(\mathbf{y}) \times \mathbf{n}(\mathbf{z}) \phi(\mathbf{z}) d\sigma(\mathbf{z}),$$

Please cite this article in press as: O. Bruno et al., Electromagnetic integral equations requiring small numbers of Krylov-subspace iterations, J. Comput. Phys. (2009), doi:10.1016/j.jcp.2009.05.020

which can easily be seen to equal the right-hand side of (36).) We can recast the identity (36) in the form

$$(\mathbf{n}\times\mathbf{S}_K)\circ\Pi_{\nabla_\Gamma} = -\overrightarrow{\operatorname{curl}}_\Gamma S_K \Delta_\Gamma^{-1}\operatorname{div}_\Gamma + S_2\Delta_\Gamma^{-1}\operatorname{div}_\Gamma, \tag{37}$$

where S_2 is the second operator on the right-hand side of Eq. (36). The kernel of the operator S_2 equals the kernel of the double layer potential, and, thus, S_2 is a smoothing operator (it maps H^s into H^{s+1} [19,22]). Hence, $S_2\Delta_\Gamma^{-1}\operatorname{div}_\Gamma$ maps $H_{\operatorname{div}}^{m-\frac{1}{2}}(\Gamma)\to H^{m+\frac{5}{2}}(TM(\Gamma))$ since another two orders of regularity are gained from the operator $\Delta_\Gamma^{-1}\operatorname{div}_\Gamma$ (note that $\phi\in H^{m+3/2}(\Gamma)$ for $\mathbf{a}\in H_{\operatorname{div}}^{m-1/2}(\Gamma)$!). Substituting (37) on the right-hand side of (7) and taking into account the identity $\operatorname{div}_\Gamma \underset{\Gamma}{\overrightarrow{\operatorname{curl}}} = 0$ together with Eqs. (34) and (35), we see that the operator

$$[\mathcal{T}\circ(\mathbf{n}\times S_K)]\circ\Pi_{\nabla_\Gamma} \equiv S_3 = ik(\mathbf{n}\times\mathbf{S}_k)\circ(\mathbf{n}\times\mathbf{S}_K)\circ\Pi_{\nabla_\Gamma} + \frac{i}{k}\mathcal{T}_{11}\operatorname{div}_\Gamma(S_2\Delta_\Gamma^{-1}\operatorname{div}_\Gamma) \tag{38}$$

is a continuous operator $S_3 : H_{\operatorname{div}}^{m-\frac{1}{2}}(\Gamma)\to H^{m+\frac{3}{2}}(TM(\Gamma))$, and thus is compact from $H_{\operatorname{div}}^{m-\frac{1}{2}}(\Gamma)$ into itself.

We now study, in turn, the action of the composition $\mathcal{T}\circ(\mathbf{n}\times\mathbf{S}_K)$ on rotational vector fields. To do this, we first note that

$$\mathbf{n}\times\mathbf{S}_K = \mathbf{n}\times\mathbf{S}_k + S_4, \tag{39}$$

where on account of the Taylor expansion of $G_K - G_k$ [22], the operator S_4 is regularizing by two orders, that is, S_4 is a continuous operator $S_4 : H^s(TM(\Gamma))\to H^{s+2}(TM(\Gamma))$. Since $(\mathbf{n}\times\mathbf{S}_k)\left(\overrightarrow{\operatorname{curl}}_\Gamma\psi\right) = \frac{1}{ik}\mathcal{T}\left(\overrightarrow{\operatorname{curl}}_\Gamma\psi\right)$ $(\operatorname{div}_\Gamma\overrightarrow{\operatorname{curl}}_\Gamma = 0)$ we obtain the relation complementary to (38):

$$[\mathcal{T}\circ(\mathbf{n}\times\mathbf{S}_K)]\circ\Pi_{\underset{\operatorname{curl}_\Gamma}{\longrightarrow}} = \frac{1}{ik}[\mathcal{T}\circ\mathcal{T}]\circ\Pi_{\underset{\operatorname{curl}_\Gamma}{\longrightarrow}} + S_5, \tag{40}$$

where $S_5 = -\mathcal{T}(S_4\Delta_\Gamma^{-1}\operatorname{curl}_\Gamma) : H^s(TM(\Gamma))\to H^{s+2}(TM(\Gamma))$ is a continuous operator, and, hence, compact from $H_{\operatorname{div}}^{m-\frac{1}{2}}(\Gamma)$ into itself. Using Calderón's identities (22) and the fact that for smooth Γ the magnetic field operator $\mathcal{K}$ is compact from $H_{\operatorname{div}}^{m-\frac{1}{2}}(\Gamma)$ to itself, we obtain from (40)

$$[\mathcal{T}\circ(\mathbf{n}\times\mathbf{S}_K)]\circ\Pi_{\underset{\operatorname{curl}_\Gamma}{\longrightarrow}} = \frac{i}{4k}\Pi_{\underset{\operatorname{curl}_\Gamma}{\longrightarrow}} + S_6, \tag{41}$$

where S_6 is compact from $H_{\operatorname{div}}^{m-\frac{1}{2}}(\Gamma)$ to itself.

Finally, we study the action of the operator $\mathcal{T}\circ(\mathbf{n}\times\mathbf{S}_K)$ on harmonic vector fields, see Remark 3.2. Since such vector fields are divergence free and the space of harmonic fields is itself finite-dimensional (its dimension equals twice the first Betti number associated to Γ), the argument leading to (41) applies in this case as well, and we thus obtain

$$[\mathcal{T}\circ(\mathbf{n}\times\mathbf{S}_K)]\circ\Pi_{\nabla_\Gamma\cap\underset{\operatorname{curl}_\Gamma}{\longrightarrow}} = \frac{i}{4k}\Pi_{\nabla_\Gamma\cap\underset{\operatorname{curl}_\Gamma}{\longrightarrow}} + S_7, \tag{42}$$

where $\Pi_{\nabla_\Gamma\bigcap\underset{\Gamma}{\overrightarrow{\operatorname{curl}}}}$ denotes the projection onto the space of harmonic vector fields and S_7 is a compact operator from $H_{\operatorname{div}}^{m-\frac{1}{2}}(\Gamma)$ to itself.

Eqs. (38), (41) and (42) tell us that, up to compact operators, the composition $\mathcal{T}\circ(\mathbf{n}\times\mathbf{S}_K)$ equals $i/(4k)$ times the sum of the projections onto the spaces of surface rotationals and harmonic vector fields. Since $\mathcal{K} : H_{\operatorname{div}}^{m-\frac{1}{2}}(\Gamma)\to H_{\operatorname{div}}^{m+\frac{1}{2}}(\Gamma)$ is a compact operator from $H_{\operatorname{div}}^{m-\frac{1}{2}}(\Gamma)$ to itself, we obtain the claimed relation (33).

Having established that the operator underlying the formulation (20) equals the sum of an invertible operator and a compact operator in the space $H_{\operatorname{div}}^{m-\frac{1}{2}}(\Gamma)$, we will prove next that the choice $K = ik_1, k_1\geqslant 0$, renders the operators in (20) injective and thus invertible as a result of the Fredholm alternative; this will conclude the proof of the Theorem. To establish injectivity, let $\mathbf{a}$ be a solution of Eq. (20) with $\mathbf{E}^i = 0$. It follows that the electromagnetic field $(\mathbf{E}^s, \mathbf{H}^s)$ defined by (18) and (19) is an outgoing solution to the Maxwell equations in the unbounded domain $\mathbf{R}^3\setminus D$ whose boundary values $\mathbf{E}_+^s$ on Γ satisfy the homogeneous conditions $\mathbf{n}\times\mathbf{E}_+^s = \mathbf{0}$. In view of the uniqueness of radiating solutions for exterior Maxwell problems [12] we obtain $\mathbf{E}^s = \mathbf{H}^s = \mathbf{0}$ identically in $\mathbf{R}^3\setminus D$. The standard jump relations of vector layer potentials then show that the limiting values of the electric field defined by (18) and (19) as $\mathbf{x}$ approaches Γ from the interior of D satisfy the relations

$$-\mathbf{n}\times\mathbf{E}_-^s = \mathbf{a}, \quad -\mathbf{n}\times\operatorname{curl}\mathbf{E}_-^s = i\xi k^2\mathbf{n}\times\mathbf{S}_K\mathbf{a}, \text{ on } \Gamma.$$

Taking the scalar product of the second of these relations with the conjugate of the first one, using standard vector relations, integrating over Γ and appealing to the divergence theorem gives

$$i\xi k^2\int_\Gamma(\mathbf{S}_K\mathbf{a})\cdot\bar{\mathbf{a}}\,d\sigma = \int_\Gamma\mathbf{n}\times\bar{\mathbf{E}}_-^s\cdot\operatorname{curl}\mathbf{E}_-^s\,d\sigma = \int_D\{|\operatorname{curl}\mathbf{E}^s|^2 - k^2|\mathbf{E}^s|^2\}d\mathbf{x}. \tag{43}$$

Thus, denoting $\{\mathbf{S}_K\mathbf{a},\mathbf{a}\} = \int_\Gamma(\mathbf{S}_K\mathbf{a})\cdot\bar{\mathbf{a}}\,d\sigma$, if $\mathbf{S}_K$ satisfies the coercivity property

"$\{\mathbf{S}_K\mathbf{a},\mathbf{a}\}\geqslant 0$, and $\{\mathbf{S}_K\mathbf{a},\mathbf{a}\} = \mathbf{0}$ iff $\mathbf{a} = \mathbf{0}$"

Please cite this article in press as: O. Bruno et al., Electromagnetic integral equations requiring small numbers of Krylov-subspace iterations, J. Comput. Phys. (2009), doi:10.1016/j.jcp.2009.05.020

then Eq. (43) implies that $\mathbf{a} = \mathbf{0}$ and the operator integral operator in Eq. (20) is injective. For a general surface Γ the coercivity property is satisfied in $H^{m-\frac{1}{2}}_{\mathrm{div}}(\Gamma)$ for wavenumbers $K = ik_1$ [22, p. 269]: the acoustic single-layer operators S_{ik_1} are coercive on $H^{m-\frac{1}{2}}(\Gamma)$. □

We now turn to the proof of existence and uniqueness of solution for Eq. (21); the proof is based on duality arguments.

Theorem 3.2. *Let $\mathcal{R} = \mathbf{S}_K$. Then the operator on the left-hand side of* Eq. (21) *satisfies*

$$\frac{I}{2} - \mathcal{K} + \xi k(\mathbf{n}\times\mathbf{S}_K)\circ\mathcal{T} \sim \left(\frac{1}{2}+\frac{i\xi}{4}\right)\Pi_{\nabla_\Gamma} + \frac{1}{2}\Pi_{\underrightarrow{\mathrm{curl}\,\Gamma}} + \left(\frac{1}{2}+\frac{i\xi}{4}\right)\Pi_{\nabla_\Gamma\bigcap\underrightarrow{\mathrm{curl}\,\Gamma}}. \tag{44}$$

Further, for $K = ik_1$, $k_1 \geqslant 0$, and $\xi > 0$, Eq. (21) *admits one and only one solution in the space $H^{m-\frac{1}{2}}_{\mathrm{div}}(\Gamma)$ for any integer $m \geqslant 0$.*

Proof. We use the duality relations [13, p. 171]

$$\begin{aligned}\{\mathcal{K}\mathbf{u},\mathbf{v}\} &= \{\mathbf{u},\mathbf{n}\times\mathcal{K}(\mathbf{n}\times\mathbf{v})\},\\ \{\mathcal{T}(\mathbf{n}\times\mathbf{u}),\mathbf{v}\} &= \{\mathbf{u},\mathcal{T}(\mathbf{n}\times\mathbf{v})\}\end{aligned} \tag{45}$$

of the operators $\mathcal{K}$ and $\mathcal{T}$ with respect to the bilinear form $\{\mathbf{u},\mathbf{v}\} = \int_\Gamma \mathbf{u}\cdot\bar{\mathbf{v}}\,d\sigma$. Using the fact that $\mathbf{S}_K = \mathbf{S}_{ik_1}$ is self-adjoint with respect to the bilinear form $\{\cdot,\cdot\}$, we obtain as an immediate consequence of the previous formulas that

$$\{\mathcal{T}(\mathbf{n}\times\mathbf{S}_K\mathbf{u}),\mathbf{v}\} = -\{\mathbf{u},\mathbf{n}\times[(\mathbf{n}\times\mathbf{S}_K)\circ\mathcal{T}](\mathbf{n}\times\mathbf{v})\}, \tag{46}$$

which leads to

$$\mathrm{DCFIE\text{-}R}_K = -\mathbf{n}\times[(\mathrm{ICFIE\text{-}R}_K)^*(\mathbf{n}\times\cdot)]. \tag{47}$$

Clearly, (47) and (33) give (44). Finally, the invertibility of DCFIE-R_K follows from (47) and the invertibility of ICFIE-R_K. □

3.3. Choice of parameters

Consideration of a wide range of numerical experiments has suggested that the parameter values

$$K = ik/2, \quad \xi = 1 \tag{48}$$

yield excellent rates of convergence for the Krylov subspace solvers: such parameter values can lead to significant reductions in iteration numbers over those required by the un-regularized equations as well as equations obtained from previous preconditioning strategies.

The corresponding choice of the coupling parameter η in the definition of the classical CFIE (17) was discussed in [20]. There it was established that

$$\eta = \frac{1}{k} \tag{49}$$

yields the lowest condition number for the continuous integral operator in the case of the unit sphere; we used this value of η to obtain all of the CFIE numerical results presented in this paper.

Remark 3.3. Our experiments indicate that the parameter η does not have a dramatic impact either on the spectral properties of the CFIE, or on the numbers of iterations required in a GMRES solution of this integral equation. On the other hand, since the eigenvalues of the integral operators (24) and (25) cluster around points in the complex plane away from zero and infinity, the choice of the corresponding parameters K and ξ greatly influence the spectral properties of these operators, and, consequently, the numbers of iterations required for solution of the corresponding discrete versions.

Having completed our introduction of regularizing operators we now present a high-order numerical method for the solution of the resulting regularized integral Eq. (20).

4. Numerical implementation: a Nyström approach

In order to avoid the exceedingly costly evaluation of the kernels of the composite operators in Eqs. (20) and (21), our implementation obtains the composition of the operators through subsequent application of high-order-accurate discretized versions of the operators $\mathcal{T}$ and $\mathcal{R}$. In what follows we detail our methodology for evaluation of the action of such discrete operators on a given vector; the overall solution is ultimately obtained by means of the iterative solver GMRES [28].

Our strategy for evaluation of the relevant discrete integro-differential operators relies on use of *local coordinate charts* together with *fixed* and *floating* partitions of unity (POU), as proposed in [7] for the related problem of soft acoustic scattering. The present context requires certain reformulations of the operators introduced in the previous sections, as well as significant extensions of methods [7] to allow for differentiations of first and second order of the integral equation unknowns, as discussed in what follows.

Please cite this article in press as: O. Bruno et al., Electromagnetic integral equations requiring small numbers of Krylov-subspace iterations, J. Comput. Phys. (2009), doi:10.1016/j.jcp.2009.05.020

4.1. Integral operators

We express both the magnetic integral operator $\mathcal{K}$ and the electric integral operator $\mathcal{T}$ in terms of integrals that only involve weakly singular kernels. The procedure is rather direct for the operator $\mathcal{K}$: since $\mathbf{a}$ is a tangential vector field, simple manipulations on Eq. (6) lead to the expression

$$(\mathcal{K}\mathbf{a})(\mathbf{x}) = \int_\Gamma \left((\mathbf{n}(\mathbf{x}) - \mathbf{n}(\mathbf{y})) \cdot \mathbf{a}(\mathbf{y}) \nabla_{\mathbf{y}} G_k(\mathbf{x}-\mathbf{y}) + \frac{\partial G_k(\mathbf{x}-\mathbf{y})}{\partial \mathbf{n}(\mathbf{x})} \mathbf{a}(\mathbf{y}) \right) d\sigma(\mathbf{y}), \tag{50}$$

which, in view of the smoothness of the surface Γ, only involves weakly singular kernels. Using integration by parts [22] on the second term in Eq. (7) and second-order derivatives of $\mathbf{a}$, in turn, the operator $\mathcal{T}$ can also be recast in a form that involves only weakly singular kernels:

$$\begin{aligned}(\mathcal{T}\mathbf{a})(\mathbf{x}) = {} & ik\, \mathbf{n}(\mathbf{x}) \times \int_\Gamma G_k(\mathbf{x}-\mathbf{y}) \mathbf{a}(\mathbf{y}) d\sigma(\mathbf{y}) - \frac{i}{k} \int_\Gamma (\mathbf{n}(\mathbf{y}) - \mathbf{n}(\mathbf{x})) \times \nabla_{\mathbf{x}} G_k(\mathbf{x}-\mathbf{y}) \mathrm{div}_\Gamma \mathbf{a}(\mathbf{y}) d\sigma(\mathbf{y}) \\ & - \frac{i}{k} \int_\Gamma G_k(\mathbf{x}-\mathbf{y}) \overrightarrow{\mathrm{curl}}_\Gamma \mathrm{div}_\Gamma \mathbf{a}(\mathbf{y}) d\sigma(\mathbf{y}) = ik \left(\mathbf{n} \times \mathbf{S}_k \mathbf{a} - \frac{1}{k^2} \mathcal{T}_1 \mathbf{a} \right).\end{aligned} \tag{51}$$

4.2. Surface representation and discretization

Following [7], the smooth bounded manifold Γ is covered by a number of overlapping coordinate patches $\mathcal{P}^\ell$, $\ell = 1, \ldots, L$ of appropriate sizes, where each patch $\mathcal{P}^\ell$, which is an open set in Γ, is the image of a planar coordinate open set $\mathcal{H}^\ell$ via the local-coordinate regular parametrization

$$\mathbf{x}^\ell = \mathbf{x}^\ell(u^\ell, v^\ell) \quad \text{for } (u^\ell, v^\ell) \in \mathcal{H}^\ell, \quad \ell = 1, \ldots, L.$$

Together with the coordinate patches that cover the manifold Γ a subordinate partition of unity $\{w^\ell(\mathbf{x}),\ \ell = 1, \ldots, L\}$ is used, with the usual properties: each w^ℓ is smooth, non-negative, compactly supported in $\mathcal{P}^\ell$, and $\sum_{\ell=1}^L w^\ell = 1$ throughout Γ.

The discretization of the densities $\mathbf{a}^\ell(u^\ell, v^\ell)$ for $\ell = 1, \ldots, L$ is obtained by means of an equidistant *Cartesian* sets of nodes (u_n^ℓ, v_m^ℓ) within $\mathcal{H}^\ell$ and corresponding nodal values $\mathbf{a}_{n,m}^\ell$.

4.3. Differentiation and integration

The *fixed* POU mentioned above can be used to reduce the evaluation of the surface integrals defining the operators $\mathcal{K}$ and $\mathcal{T}$ to planar integrals over the sets $\mathcal{H}^\ell$. The resulting integrands involve products of various weakly-singular kernels, Jacobian determinants J^ℓ, the POU functions w^ℓ and either the unknown density $\mathbf{a}$ or its derivatives of first or second order—which arise in the (u^ℓ, v^ℓ) coordinate expressions [16] of the differential operators ∇_Γ and div_Γ. Thus, each one of the integral operators $\mathcal{L}$ we need to consider ($\mathcal{L} = \mathcal{K}, \mathcal{L} = \mathcal{T}$ and $\mathcal{L} = \mathcal{R}_K$) can be expressed as a sums of integrals of the form

$$(\mathcal{L}\mathbf{a})(\mathbf{x}) = \sum_{\ell=1}^L \int_{\mathcal{H}^\ell} G(k, \mathbf{x}, \mathbf{x}^\ell(u^\ell, v^\ell), \mathbf{n}^\ell(u^\ell, v^\ell)) w^\ell(\mathbf{x}(u^\ell, v^\ell)) J^\ell(u^\ell, v^\ell) \cdot \sum_{0 \leqslant \alpha+\beta \leqslant 2} c_{\alpha\beta}(u^\ell, v^\ell) \partial_{u^\ell}^\alpha \partial_{v^\ell}^\beta \mathbf{a}^\ell(u^\ell, v^\ell)) du^\ell\, dv^\ell, \tag{52}$$

where $c_{\alpha\beta}$ are coefficients arising from the coordinate forms of the differential operators mentioned above.

Since the products $W^\ell(u^\ell, v^\ell) = w^\ell(u^\ell, v^\ell) J^\ell(u^\ell, v^\ell)$ vanish to high order at the boundary of the integration domain $\mathcal{H}^\ell$, they can be extended by periodicity to smooth *periodic* functions defined in the whole plane—thus fitting the high-order trapezoidal-rule-integration and Fourier-series-interpolation paradigm [7]. As shown in what follows, further, this setup can be used to enable high-order evaluation of derivatives of the smooth but generally *non-periodic* densities $\mathbf{a}^\ell$.

Indeed, for the first-order derivatives with respect to u^ℓ we can write

$$W^\ell(u^\ell, v^\ell) \partial_{u^\ell} \mathbf{a}^\ell(u^\ell, v^\ell) = W^\ell(u^\ell, v^\ell)^{1-\delta} \{ \partial_{u^\ell} [W^\ell(u^\ell, v^\ell)^\delta \mathbf{a}^\ell(u^\ell, v^\ell)] - \mathbf{a}^\ell(u^\ell, v^\ell) \partial_{u^\ell} (W^\ell(u^\ell, v^\ell)^\delta) \}, \tag{53}$$

for an arbitrary $0 < \delta \leqslant 1$, with a similar formula for the v^ℓ derivatives. The second-order derivatives can be obtained using this procedure twice, using each time a power $\delta \leqslant \frac{1}{2}$; we found in practice that the value $\delta = \frac{1}{4}$ yields a perfectly adequate performance. In formulas (53) the differentiation operators act on smooth and periodic functions, so that the corresponding derivatives can be obtained through differentiation of the corresponding Fourier series. For efficiency it is imperative to use FFTs for evaluation of Fourier series; further, it is preferable to utilize POUs with small derivatives: this can be arranged by allowing for substantial overlap amongst the patches $\mathcal{P}^\ell$.

With these preliminaries, the high-order quadrature rule we use for the numerical evaluation of the integrals in Eq. (52) is to a large extent identical to the one introduced in [7]. A somewhat significant difference arises in connection with the use of imaginary wavenumbers $K = ik_1$ in the regularizing operator $\mathbf{S}_K$. Indeed, for real wavenumbers k, the fundamental solution contains the oscillatory factor $e^{ik|\mathbf{R}|}$, whereas for the imaginary wavenumber ik_1 the corresponding factor is a decaying exponential $e^{-k_1|\mathbf{R}|}$. A cursory analysis of Eq. (11) in [7] and the corresponding formulae involving decaying exponentials reveals the trapezoidal/polar approach of [7] does not yield high-order accuracy for the decaying exponential integrands under

Please cite this article in press as: O. Bruno et al., Electromagnetic integral equations requiring small numbers of Krylov-subspace iterations, J. Comput. Phys. (2009), doi:10.1016/j.jcp.2009.05.020

consideration. To see this, let $s = |\mathbf{R}(\rho,\theta)|$ for a fixed θ (a radius in the polar integration technique of [7]). Clearly, the functions $\cos ks$ and $\sin ks/s$ are smooth (analytic) functions for all real values of ρ, including $\rho = 0$, while the function $e^{-k_1 s}$ is not a smooth function of ρ at $\rho = 0$. Thus, while the terms arising in the real wavenumber case $K = k$ can be treated with high-order accuracy by means of a combination of a two-dimensional Cartesian trapezoidal rule (for terms such as $\cos ks$) and a two-dimensional polar trapezoidal rule (for terms such as $\sin ks/s$), the integral of $e^{-k_1|\mathbf{R}|}$ cannot generally be evaluated with high-order accuracy by either of these approaches. (The relation $e^{-k_1|\mathbf{R}|} = (\cosh(-k_1|\mathbf{R}|) + \sinh(-k_1|\mathbf{R}|))$, which might in principle suggest that an approach similar to that associated with Eq. (11) in [7] could be utilized, gives rise to significant cancellation errors even for moderately large values of $k_1|\mathbf{R}|$, and thus cannot be generally used.) To address this difficulty we re-express the integral under consideration

$$\widetilde{L}_1(u,v,\theta) = \int_{-r_1}^{r_1} f_\ell^*(\rho,\theta)\frac{|\rho|}{|\mathbf{R}|}e^{-k_1|\mathbf{R}|}d\rho \tag{54}$$

as the sum of the integrals

$$\widetilde{L}_1(u,v,\theta) = \int_{-r_1}^{0} f_\ell^*(\rho,\theta)\frac{|\rho|}{|\mathbf{R}|}e^{-k_1|\mathbf{R}|}d\rho + \int_{0}^{r_1} f_\ell^*(\rho,\theta)\frac{|\rho|}{|\mathbf{R}|}e^{-k_1|\mathbf{R}|}d\rho,$$

each one of which can be evaluated by means of a suitable one-dimensional high-order integration method—which we take to be the composite Newton–Cotes method of order seven. This particular choice is motivated by several considerations: (1) seven is the highest order for which the Newton–Cotes with evenly spaced data method contains only positive weights, and thus avoids instabilities associated with the Runge phenomenon; (2) the order-seven Newton–Cotes formulae provides stable quadrature of a rather high order with a cost comparable to the trapezoidal quadrature; and (3) this method can be implemented as long as the single additional value of the unknown density at the target point $\mathbf{R} = 0$ is available (as it is for all the required polar-coordinate integrations in the approach [7]), besides the values of the density at evenly spaced points in the interval $[-r_1, r_1]$ required by the trapezoidal quadrature.

It must be noted that, for a given angle $\theta = \theta_i$, the target point $\mathbf{R} = 0$ can be arbitrarily positioned within the radial interval $[-r_1, r_1]$, and, thus, special consideration must be given to design a Newton–Cotes method on the unevenly spaced data points that start or end at $r = 0$. In detail, if $r_1^{(0)}, \ldots, r_1^{(P)}$ is an evenly spaced discretization of the radial interval $[-r_1, r_1]$ such that the target-point $r = 0$ lies in the open interval $(r_1^{(p)}, r_1^{(p+1)})$, $0 \leqslant p \leqslant P-1$, the discretization points $r_1^{(p)}$ and $r_1^{(p+1)}$ will be used in the Newton–Cotes formulas only if, for a suitably chosen value of the tolerance ε_{tol}, the relations

$$\frac{|r_1^{(p)}|}{r_1^{(1)} - r_1^{(0)}} \geqslant \varepsilon_{\text{tol}} \quad \text{and} \quad \frac{|r_1^{(p+1)}|}{r_1^{(1)} - r_1^{(0)}} \geqslant \varepsilon_{\text{tol}} \tag{55}$$

are satisfied. This precaution must be taken in order to eliminate very large Newton–Cotes weights and associated ill-conditioning that arise as the target point $r = 0$ is too close to one of the endpoints of the radial interval that contains it. In the case that one of the constraints (55) fails to be satisfied, the corresponding discretization point is not used in the Newton–Cotes method. In all of the numerical results of this paper the value $\varepsilon_{\text{tol}} = 0.01$ was used.

Remark 4.1. We note that, in principle, other high-order quadrature rules such as the Chebyshev or Gauss methods could be used in order to evaluate accurately integrals of the type (54). However, these alternatives would require interpolations along each radial lines in order to produce the values of the densities at the radial Chebyshev and Gauss points in addition to those already used to produce those values at evenly spaced radial points. We have found that, for accuracies of up to several digits, the Newton–Cotes approach is perfectly adequate: it achieves accuracy levels similar to those resulting from the Chebyshev and Gauss quadratures with a significantly more favorable overall computational cost, and hence this is our method of choice.

5. Numerical results

In what follows we present a collection of numerical results produced by the various types of regularized integral equations under consideration, including the un-regularized direct and indirect Eqs. (14) and (17); the corresponding regularized equations ICFIE-R_K and DCFIE-R_K (that is, Eqs. (20) and (21) with regularizing operator (23) and with regularization and coupling parameters (48)); and the Calderón regularized CFIE introduced in reference [15] with coupling parameter (49)—which in the remainder of this paper will be denoted by "CFIE [15]".

Remark 5.1. The numerical methods we use for the various integral formulations under consideration produce the necessary high-order numerical derivatives and quadratures according to the prescriptions detailed in Section 4.3. In particular, for the integral operators that involve complex wavenumbers, quadrature points not satisfying Eq. (55) with $\varepsilon_{tol} = 0.01$ are not used in the corresponding Newton–Cotes procedure.

Solutions of the linear systems arising from the discretization of these equations were obtained by means of the iterative solver GMRES [28]; the results of this section demonstrate the significant reductions in the numbers of iterations that result from use of the regularizers introduced in this text. Most of the numerical results presented in this section were obtained by

Please cite this article in press as: O. Bruno et al., Electromagnetic integral equations requiring small numbers of Krylov-subspace iterations, J. Comput. Phys. (2009), doi:10.1016/j.jcp.2009.05.020

prescribing a GMRES residual tolerance equal to 10^{-4}; the reference solutions for the scattering experiments with plane-wave incidences, in turn, resulted from finer-mesh discretizations and GMRES residual tolerances equal to either 10^{-6} or 10^{-8}.

We present results for three scattering surfaces: a sphere of radius one, an elongated ellipsoid (of principal axes 2, 0.75 and 1) and a bean-shaped body, and we consider, amongst others, scattering problems involving the wavenumbers $k = 8, 16$ and 32. For all the geometries considered these wavenumbers correspond to scatterers of 2.5λ, 5.1λ and 10.2λ in diameter, respectively. The bean shaped geometry mentioned above is described in [7]; it is given by the equation

$$\frac{x^2}{a^2(1-\alpha_3\cos\frac{\pi z}{R})}+\frac{\left(\alpha_1 R\cos\frac{\pi z}{R}\right)^2}{b^2(1-\alpha_2\cos\frac{\pi z}{R})}+\frac{z^2}{c^2}=R^2$$

with $a = 0.8, b = 0.8, c = 1, \alpha_1 = 0.3, \alpha_2 = 0.4, \alpha_3 = 0.1$ and $R = 1$. For efficiency, configurations requiring larger numbers of unknowns than those we considered in this text should be dealt with by means of adequate acceleration techniques (e.g. [7]); such cases lie beyond the scope of this paper and will be considered in our forthcoming work [9].

With exception of the bean-shaped geometry, in all of our plane-wave-incident-field examples we assumed an incident field in the form of a plane wave propagating down the z axis with polarization $(1, 0, 0)$. For the bean-shaped scatterer, in contrast, we assumed the polarization $(0, -\frac{1}{\sqrt{2}}, \frac{1}{\sqrt{2}})$ and, in order for the configuration to give rise to multiple reflections, a direction of incidence $\left(-\frac{\sqrt{3}}{3}, -\frac{\sqrt{3}}{3}, -\frac{\sqrt{3}}{3}\right)$.

For every scattering experiment we present the maximum error amongst all directions $\hat{\mathbf{x}} = \frac{\mathbf{x}}{|\mathbf{x}|}$ of the far field $\mathbf{E}_\infty(\hat{\mathbf{x}})$:

$$\mathbf{E}(\mathbf{x}) = \frac{e^{ik|\mathbf{x}|}}{|\mathbf{x}|}\left(\mathbf{E}_\infty(\hat{\mathbf{x}}) + \mathcal{O}\left(\frac{1}{|\mathbf{x}|}\right)\right) \quad \text{as} \quad |\mathbf{x}| \to \infty. \tag{56}$$

The maximum far-field error, which we denote by ε_∞,

$$\varepsilon_\infty = \max_{\hat{\mathbf{x}}} |\mathbf{E}_\infty^{\text{calc}}(\hat{\mathbf{x}}) - \mathbf{E}_\infty^{\text{ref}}(\hat{\mathbf{x}})| \tag{57}$$

was evaluated in our numerical examples as the maximum difference (over a uniform discretization of the unit sphere $|\hat{\mathbf{x}}| = 1$, containing 5766 points corresponding to six patches and 31×31 points per patch) between far fields $\mathbf{E}_\infty^{\text{calc}}$ obtained from our numerical solutions and corresponding far fields $\mathbf{E}_\infty^{\text{ref}}$ associated with reference solutions. The reference solutions we used were obtained either from exact solutions, when those are available, and from finer-mesh solutions for other cases. To obtain the latter reference solutions we used the ICFIE-R_0 using fine discretizations; specifically, 47,628 unknowns were used for the fine-mesh solutions in the case of the ellipsoid and bean configurations of diameters 2.5λ and 5.1λ (corresponding to six patches and 63×63 (u, v) discretization points per patch), and 193,548 unknowns (corresponding to six patches and 127×127 points per patch) were used for the corresponding 10.2λ ellipsoid and bean configurations.

Our first example, presented in Table 1, demonstrates the high-order nature of our algorithms. This table displays far-field errors produced by the $K = 0$ version of the CFIE-R formulation (24), for various discretizations, for the problem of scattering of an incident plane wave by a sphere of radius 2.7λ. The electromagnetic size of the problem and the samplings are identical to those in Table 4 in [7], except that twice the number of unknowns is needed here for the two-dimensional surface density that occurs in the electromagnetic case. The high-order convergence demonstrated in Table 1 is similar to that reported in Table 4 of [7] for the sound-soft case: halving the mesh-size results in accuracy improvements of up to two orders of magnitude. We used GMRES tolerances of 10^{-4} for the first two discretizations, 10^{-6} for the third and 10^{-8} for the fourth. The high-order character of the algorithm is clearly observed.

Tables 2–4, in turn, display iteration numbers and far field errors, as well as the number of iterations required by the GMRES solver to reach a relative residual of 10^{-4}, for five different integral formulations and for the various scattering shapes and sizes we consider. (The formulation CFIE-mod[15], which was not considered earlier in this text, together with associated accuracy considerations, are discussed below in this section.) For each one of the scattering surfaces (sphere, ellipsoid and bean) we used 8748, 36,300 and 147,852 unknowns for the scattering problems of diameters 2.5λ, 5.1λ and 10.2λ, respectively—corresponding to six patches and 27×27, 55×55 and 111×111 discretization points per patch, respectively. Our numerical experiments indicate that the number of iterations and the accuracy of the implementation of the unpreconditioned ICFIE formulation (17) are virtually identical to those produced through the implementation of the unpreconditioned CFIE formulation (14); consequently, in Tables 2–4 we do not include results for the ICFIE formulation.

Table 1
Convergence study. Scattering from a sphere of radius equal to 2.7λ, using the ICFIE-R_K formulation (24) with $K = 0$.

Patches	Unknowns	Discretization density	ϵ_∞
$6 \times 15 \times 15$	2700	3 per λ	1.8×10^{-2}
$6 \times 31 \times 31$	11,532	6 per λ	7.9×10^{-4}
$6 \times 63 \times 63$	47,628	12 per λ	4.1×10^{-5}
$6 \times 127 \times 127$	193,548	24 per λ	5.4×10^{-7}

Please cite this article in press as: O. Bruno et al., Electromagnetic integral equations requiring small numbers of Krylov-subspace iterations, J. Comput. Phys. (2009), doi:10.1016/j.jcp.2009.05.020

Table 2
Scattering by spheres 2.5λ, 5.1λ and 10.2λ in diameter; solutions obtained using 8748, 36,300 and 147,852 unknowns, respectively, and a number "It." of GMRES iterations. Residual tolerance = 10^{-4}.

Size	ICFIE-R_K		DCFIE-R_K		CFIE [15]		CFIE-mod [15]		CFIE	
	It.	ε_∞	It.	ε_∞	It.	ε_∞	It.	ε_∞	It.	ε_∞
2.5λ	11	8.2×10^{-4}	11	7.0×10^{-4}	13	1.9×10^{-3}	11	1.5×10^{-3}	32	6.0×10^{-4}
5.1λ	12	4.6×10^{-4}	12	1.2×10^{-4}	16	2.5×10^{-3}	14	7.0×10^{-4}	33	3.2×10^{-4}
10.2λ	14	2.9×10^{-4}	14	2.8×10^{-4}	19	2.9×10^{-3}	18	4.8×10^{-4}	35	5.7×10^{-4}

Table 3
Scattering by ellipsoids 2.5λ, 5.1λ and 10.2λ in diameter; solutions obtained using 8748, 36,300 and 147,852 unknowns, respectively, and a number "It." of GMRES iterations. Residual tolerance = 10^{-4}.

Size	ICFIE-R_K		DCFIE-R_K		CFIE [15]		CFIE-mod [15]		CFIE	
	It.	ε_∞	It.	ε_∞	It.	ε_∞	It.	ε_∞	It.	ε_∞
2.5λ	13	4.1×10^{-4}	12	3.6×10^{-4}	14	1.6×10^{-3}	14	1.8×10^{-3}	49	6.2×10^{-4}
5.1λ	12	1.3×10^{-4}	12	9.5×10^{-5}	16	4.4×10^{-4}	15	3.5×10^{-4}	52	1.4×10^{-4}
10.2λ	13	1.2×10^{-4}	13	1.0×10^{-4}	23	6.0×10^{-4}	20	3.9×10^{-4}	55	1.7×10^{-4}

Table 4
Scattering by bean-shaped surfaces 2.5λ, 5.1λ and 10.2λ in diameter; solutions obtained using 8748, 36,300 and 147,852 unknowns, respectively, and a number "It." of GMRES iterations. Residual tolerance = 10^{-4}.

Size	ICFIE-R_K		DCFIE-R_K		CFIE[15]		CFIE-mod[15]		CFIE	
	It.	ε_∞	It.	ε_∞	It.	ε_∞	It.&ε_∞	It.	ε_∞	
2.5λ	13	8.5×10^{-4}	12	9.2×10^{-4}	18	1.6×10^{-3}	15	1.5×10^{-3}	44	1.0×10^{-3}
5.1λ	12	1.6×10^{-4}	12	1.4×10^{-4}	21	1.4×10^{-3}	18	7.6×10^{-4}	48	1.3×10^{-3}
10.2λ	14	1.6×10^{-4}	14	1.6×10^{-4}	24	2.5×10^{-3}	22	5.2×10^{-4}	54	2.4×10^{-3}

The various numerical results presented in this section support the main claims of this paper: the new regularized integral equations give rise to significant reductions in the number of iterations required by the GMRES solver, and the high-order Nyström implementation we propose for their solution gives rise to highly accurate solutions: the overall accuracy of the solutions of the integral equation formulations ICFIE-R_K and DCFIE-R_K is comparable to (or better than) the error corresponding to ICFIE or CFIE. Since the computational time required by a matrix–vector product for the discrete regularized equations is approximately 1.6 times that required by the classical CFIE for the same discretization, the gains in run times resulting from the new regularized equations are very significant. These improvement levels contrast with those obtained from the method [15] which, using of the regularizing operator $\mathcal{T}$, requires computational time per iteration of the order 2.5 times those required by ICFIE or CFIE—in addition to requiring larger numbers of iterations than the new formulations. The combined effect of these CFIE[15] additional costs in the context of our test cases is demonstrated in Table 6.

(The method introduced in [15] uses the operator $\mathbf{n}\times\mathcal{R}=\mathcal{T}(ik)$ as a regularizer: the equation CFIE [15] introduced in that contribution is given by

$$\frac{\mathbf{J}}{2}-\mathcal{K}\mathbf{J}+ik^2\,\mathcal{T}(ik)\circ\mathcal{T}(k)\mathbf{J}=\mathbf{n}\times\mathbf{H}^i-ik^2\mathcal{T}(ik)(\mathbf{n}\times\mathbf{E}^i). \tag{58}$$

The numerical examples presented in [15] concern the very-low-frequency end of the spectrum; no information was provided in that text with regards to the performance of Eq. (58) in the intermediate or high-frequency regime. We thus undertook the task of implementing and testing the formulation (58). We found that, as pointed out in [15], in order to produce an adequate implementation of CFIE [15] it is necessary to account explicitly for the fact that the composition of the operators $\mathcal{T}_1(k)$ and $\mathcal{T}_1(ik)$ vanishes—a failure to account for that cancellation results in low accuracies and iteration numbers that are up to four times larger than the CFIE [15] numbers reported in the Tables 2–4. Even after such explicit cancellations, how-

Table 5
Solution of a problem of scattering from a sphere of radius equal to 2.7λ demonstrating the high-order convergence of our implementations of the various regularized equations.

Unknowns	Discretization density	CFIE [15]	CFIE-mod [15]	ICFIE-$R_{ik/2}$	ICFIE-R_{ik}
2700	3 per λ	7.8×10^{-2}	7.7×10^{-2}	7.7×10^{-2}	7.3×10^{-2}
11,532	6 per λ	3.4×10^{-3}	2.0×10^{-3}	1.9×10^{-3}	3.1×10^{-3}
47,628	12 per λ	3.4×10^{-4}	1.4×10^{-4}	7.7×10^{-5}	3.1×10^{-4}

Please cite this article in press as: O. Bruno et al., Electromagnetic integral equations requiring small numbers of Krylov-subspace iterations, J. Comput. Phys. (2009), doi:10.1016/j.jcp.2009.05.020

Table 6
Performance of various formulations. Scattering from objects of diameter equal to 5.4λ, point source inside, using the CFIE formulation (14) with coupling parameter $\eta = 1/k$, the ICFIE-R_K, formulation (24) with $K = k/2$ and $\xi = 1$, the ICFIE-R formulations (58) introduced in [15], and the modified version of the latter given by Eq. (59).

Scatterer	Unknowns	CFIE (14)		ICFIE-R_K (24)		CFIE [15] & CFIE-mod [15]		
		It./Tot. time	Time/It.	It./Tot. time	Time/It.	It./Tot. time (58)	It./Tot. time (59)	Time/It.
Sphere	10,800	12/5 m 21 s	26.75 s	8/5 m 36 s	42.0 s	13/15 m 21 s	7/8 m 15 s	70.84 s
Sphere	37,632	11/36 m 8 s	197.09 s	7/35 m 44 s	306.28 s	9/78 m 23 s	7/60 m 58 s	522.55 s
Ellipsoid	10,800	29/12 m 30 s	25.86 s	12/8 m 23 s	41.91 s	22/26 m 16 s	16/19 m 6 s	71.63 s
Ellipsoid	37,632	37/112 m 50 s	182.97 s	11/56 m 36 s	308.73 s	21/182 m 39 s	15/130 m 28 s	521.85 s
Bean	10,800	33/18 m 34 s	33.76 s	13/10 m 35 s	48.85 s	21/28 m 50 s	19/26 m 13 s	82.38 s
Bean	37,632	42/155 m 55 s	222.74 s	12/65 m 45 s	328.75 s	19/178 m 22 s	16/150 m 12 s	563.26 s

ever, CFIE [15] gives rise to lower accuracies than those provided by the new CFIE-R_K and ICFIE-R_K formulations; see Tables 2–5. We have traced the source of the reduced CFIE [15] accuracy to the fact that, while our formulations are based on use of the regularizing wavenumber $K = ik/2$, the formulation (58) uses the parameter value $K = ik$ (in its own regularizing operator, which is different from that used in the CFIE-R approach). To demonstrate this finding we present in Tables 2–5 an additional set of results that were produced by a modified version of CFIE [15], that we label CFIE-mod [15], which is given by

$$\frac{\mathbf{J}}{2} - \mathcal{K}\mathbf{J} + \frac{ik^2}{2}\,\mathcal{T}(ik/2)\circ\mathcal{T}(k)\mathbf{J} = \mathbf{n}\times\mathbf{H}^i - \frac{ik^2}{2}\mathcal{T}(ik/2)(\mathbf{n}\times\mathbf{E}^i); \tag{59}$$

the only difference between Eqs. (58) and (59) is that the regularizer in the latter uses the parameter $K = ik/2$ instead of the value $K = ik$ used in the former. The results in Tables 2–5 show that use of the formulation CFIE-mod [15] yields far-field errors comparable to the ones obtained from our CFIE-R_K and ICFIE-R_K formulations ($K = ik/2$). Yet the CFIE-mod [15] still requires significantly higher overall computing costs than the new CFIE-R_K and ICFIE-R_K formulations for a given accuracy, as discussed in what follows.)

Table 6 presents a suggestive comparison between the performance of the CFIE formulation (14) and the regularized formulations (24), (58) and (59) for three scattering configurations, namely, the unit sphere, elongated ellipsoid and bean-shaped scatterer of diameters equal to 5.4λ. In each case we run the solvers using two different discretizations, consisting of 10,800 ($2\times 6\times 30\times 30$) and 37,632 ($2\times 6\times 56\times 56$) discretization points, with the GMRES residual tolerance set to 10^{-4}. The boundary conditions were taken to equal the field of an electric point source located inside the scatterers at a distance 0.2 from the origin and 10° off the vertical axis. (For such boundary conditions the exact solution, which equals the point-source field itself, can be used to determine the accuracy of the numerical solution. Note, however, the anomalously small numbers of iterations required for the ICFIE formulation *in the case of the spherical scatterer* under the present point-source-inside boundary conditions: compare Table 2.) Table 6 displays the total (overall) computational time, the time per iteration, and the number of iterations required for each individual numerical experiment. The far-field errors incurred by the three versions were comparable, i.e. of order 10^{-3} for the coarser discretizations and of order 10^{-4} for the finer discretizations, respectively. Once again we note that the modified formulation (59) produces results about as accurate as those obtained by the formulation (24) with $K = ik/2$. Notably, both the CFIE [15] and CFIE-mod [15] formulations require *longer overall computing times* than the unregularized CFIE, whereas our CFIE-R_K approaches lead to significant overall time savings over those required by the CFIE.

The computational times reported resulted from a C++ numerical implementation of our algorithm, as described in the previous sections, that was run on a desktop computer with a single Intel (R) Xeon processor at 2.33 GHz with 2 GB RAM, running GNU/Linux, and using the GNU/gcc compiler, the PETSC 3.0 library for the fully complex implementation of GMRES, and the FFTW3 library for evaluation of FFTs. The computational times required by one matrix–vector product for the cases of the sphere and the ellipsoid are almost identical. The slightly larger computational times required by the bean-shaped cases arises from our use of larger overlaps between the patches in the chart atlas, which is necessary in this case to achieve the same level of accuracy as for the sphere and ellipsoid configurations.

Two additional observations can be drawn from the results presented in Table 6: (1) a matrix–vector product resulted from discretization of the formulations (24) is on average at most 1.6 more computationally expensive than the matrix–vector product for the CFIE formulation (16) at the same level of discretization; and (2) a matrix–vector product resulted from discretization of the formulations (58) is on average at most 2.5 more computationally expensive than the matrix–vector product for the CFIE formulation (16) at the same level of discretization but with some losses of accuracy and larger iteration numbers. We also mention that in the same computational architecture, the computational cost of one matrix–vector product of the CFIE formulation (16) is only two times more expensive than the cost of one matrix–vector product for the combined field formulation for acoustic Dirichlet problem using the algorithm introduced in [7].

To demonstrate the stability of our ICFIE-R_K formulation (24) as the frequencies are varied, finally, in Fig. 1 we display the number of iterations required to reach a GMRES residual of 10^{-4} using the ICFIE-R_K formulation (24) with $K = ik/2$ and $\xi = 1$: the left and right portions of this figure present results corresponding, respectively, to two different types of incident fields, namely, point-source incidence of the kind used in Table 6, and plane-wave incidence of the type used in Tables 2–4. For each

Please cite this article in press as: O. Bruno et al., Electromagnetic integral equations requiring small numbers of Krylov-subspace iterations, J. Comput. Phys. (2009), doi:10.1016/j.jcp.2009.05.020

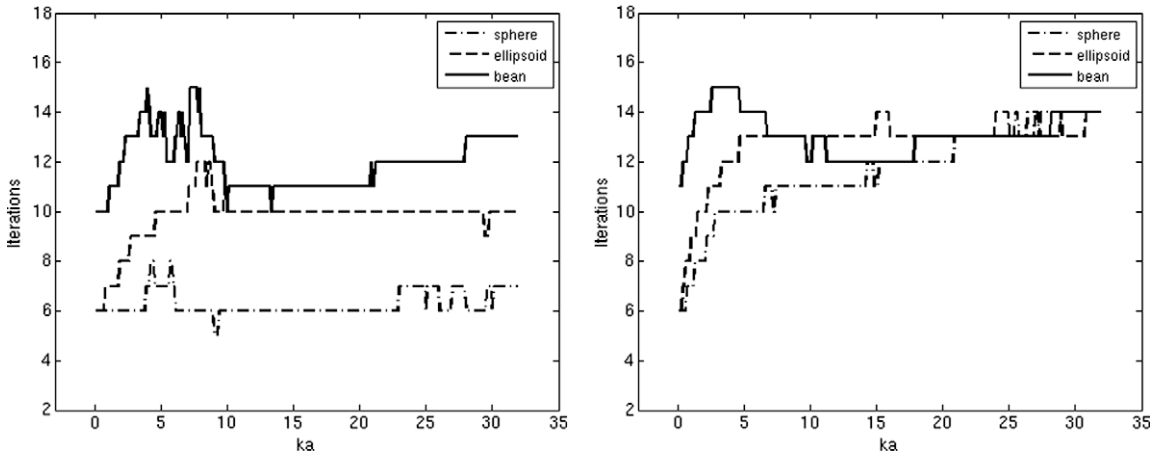

Fig. 1. Numbers of iterations to 10^{-4} GMRES residuals for the ICFIE-R_K formulations (24) with $\xi = 1$ and $K = k/2$, for three geometries: unit sphere, ellipsoid and bean-shaped geometry. Point-source and plane-wave incident fields were used in the left and right figures, respectively. For the left figure the far field error was computed through comparison with the exact solution, and found to be of the order of 10^{-4}. The figures display the iteration numbers for the sequence of 320 wavenumbers $k = 0.1, 0.2, \ldots, 32$ and corresponding discretizations that deliver far-field errors of order 10^{-4}. Clearly, the unique solvability established in Theorems 3.1 and 3.2 is realized in practice: no resonant frequencies were found.

geometrical configuration and incidence type we present results for 320 wavenumbers k ranging from 0.1 to 32 spaced 0.1 apart. We used discretizations similar to those used otherwise throughout this section, so that 4 digits of accuracy were obtained in the far-field when compared with the exact solutions for point-source incidences or with refined discretizations for plane-wave incidences. Clearly no resonant frequencies exist, in accordance with the existence and uniqueness proof presented in Section 3.2.

The results of this section demonstrate the excellent properties of the new regularized integral equations and the associated implementation described in Section 4: the new equations are well conditioned, and they can produce highly accurate solutions in significantly shorter computing times and smaller numbers of iterations than previous approaches.

6. Conclusions

We have introduced novel classes Regularized Combined Field Integral Equations formulations for the solution of Maxwell equations. The equations and high-order implementations introduced in this text provide significant improvements in accuracy and computational cost over the most competitive (unaccelerated) approaches otherwise in existence today for the treatment of problems of electromagnetic scattering by perfectly conducting surfaces. In particular, we found that the Regularized Combined Field Integral Equations ICFIE-R_K and DCFIE-R_K have excellent spectral properties, as evidenced by the reduced numbers of iteration required for convergence of the GMRES iterative solver. Corresponding low-iteration-number, high-accuracy algorithms for treatment of large electromagnetic problems (based on a combination of the main elements introduced in this text with the equivalent-source acceleration techniques originally introduced in [7] in the acoustic scattering context) will be presented in the forthcoming contribution [9].

Acknowledgments

We gratefully acknowledge support by the Air Force Office of Scientific Research and the National Science Foundation.

References

[1] R.J. Adams, Combined field integral equation formulations for electromagnetic scattering from convex geometries, IEEE Trans. Antennas Propag. 52 (2004) 1294–1303.
[2] R.J. Adams, G.S. Brown, Stabilization procedure for Electric Field Integral Equation, Electron. Lett. 35 (23) (1999) 2015–2016.
[3] F. Alouges, S. Borel, D. Levadoux, A stable well-conditioned integral equation for electromagnetism scattering, J. Comput. Appl. Math. 204 (2007) 440–451.
[4] X. Antoine, M. Darbas, Generalized Combined Field Integral Equations for the iterative solution of the three-dimensional Helmholtz equation, Math. Model. Numer. Anal. 41 (2007) 147–167.
[5] E. Bleszynski, M. Bleszynski, T. Jaroszewicz, AIM: adaptive integral method for solving large-scale electromagnetic scattering and radiation problems, Radio Sci. 31 (5) (1996) 1225–1251.
[6] S. Borel, D. Levadoux, F. Alouges, A new well-conditioned formulation of Maxwell equations in three dimensions, IEEE Trans. Antennas Propag. 53 (9) (2005) 2995–3004.
[7] O. Bruno, L. Kunyansky, Surface scattering in three dimensions: an accelerated high-order solver, R. Soc. Lond. Proc. Ser. A Math. Phys. Eng. Sci. 2016 (2001) 2921–2934.

Please cite this article in press as: O. Bruno et al., Electromagnetic integral equations requiring small numbers of Krylov-subspace iterations, J. Comput. Phys. (2009), doi:10.1016/j.jcp.2009.05.020

[8] O.P. Bruno, L. Kunyansky, A. fast, high-order algorithm for the solution of surface scattering problems: basic implementation, tests and applications, J. Comput. Phys. 169 (2001) 80–110.
[9] O. Bruno, T. Elling, C. Turc, Electromagnetic surface scattering in three dimensions: accelerated high-order solvers (in preparation).
[10] B. Carpentieri, A matrix-free two-grid preconditioner for solving boundary integral equations in electromagnetism, Computing 77 (2006) 275–296.
[11] A. Calderón, The multipole expansion of radiation fields, Arch. Rat. Mech. Anal. 3 (1954) 523–537.
[12] D. Colton, R. Kress, Integral Equation Methods in Scattering Theory, Wiley Interscience, New York, 1983.
[13] D. Colton, R. Kress, Inverse Acoustic and Electromagnetic Scattering Theory, second ed., Springer-Verlag, New York, 1992.
[14] S. Christiansen, J.C. Nédélec, A preconditioner for the Electric Field Integral Equation based on Calderón formulas, SIAM J. Numer. Anal. 40 (3) (2002) 1100–1135.
[15] H. Contopanagos, B. Dembart, M. Epton, J. Ottusch, V. Rohklin, J. Visher, S. Wandzura, Well-conditioned boundary intergal equations for three-dimensional electromagnetic scattering, IEEE Trans. Antennas Propag. 50 (12) (2002) 1824–1830.
[16] M.P. Do Carmo, Riemannian Geometry, Birkhuser, 1992.
[17] R. Harrington, J. Mautz, H-field, E-field and combined field solution for conducting bodies of revolution, Arch. Elek. Uber. (AEU) 32 (4) (1978) 157–164.
[18] C. Hazard, M. Lenoir, On the solution of the time-harmonic scattering problems for Maxwell's equations, SIAM J. Math. Anal. 27 (1996) 1597–1630.
[19] G.C. Hsiao, R.E. Kleinman, Mathematical foundations for error estimation in numerical solutions of integral equations in electromagnetics, IEEE Trans. Antennas Propag. 45 (1997) 316–328.
[20] R. Kress, Minimizing the condition number of boundary integral operators in acoustic and electromagnetic scattering, Q. J. Mech. Appl. Math. 38 (1985) 323–341.
[21] A.W. Maue, On the formulation of a general scattering problem by means of an integral equation, Z. Phys. 125 (1949) 601–618.
[22] J.C. Nédélec, Acoustic and Electromagnetic Equations, Springer Verlag, New York, 2001.
[23] J.C. Nédélec, Computation of eddy currents on a surface in $\mathbb{R}^3$ by finite element methods, SIAM J. Numer. Anal. 15 (3) (1978) 580–594.
[24] A.J. Poggio, E.K. Miller, Integral equation solutions of three-dimensional scattering problems, in: R. Mittra (Ed.), Computer Techniques for Electromagnetics, Pergamon, New York, 1973, pp. 201–210 (Chapter 4).
[25] S.M. Rao, D.R. Wilton, A.W. Glisson, Electromagnetic scattering by surfaces of arbitrary shape, IEEE Trans. Antennas Propag. 30 (3) (1982) 409–418.
[26] P.A. Raviart, J.M. Thomas, A mixed finite element method for second order elliptic problems, in: I. Galligani, E. Magenes (Eds.), Mathematical Aspects of the Finite Element Method, Lecture Notes in Mathematics, vol. 606, Springer, Berlin, 1975, pp. 292–315.
[27] V. Rokhlin, Diagonal form of translation operators for the Helmholtz equation in three dimensions, Appl. Comput. Harmon. Anal. 1 (1993) 82–93.
[28] Y. Saad, M.H. Schultz, GMRES: a generalized minimal residual algorithm for solving non-symmetric linear systems, SIAM J. Sci. Stat. Comput. 3 (7) (1986) 856–869.
[29] R. Seeley, Topics in pseudo-differential operators, in: L. Niremberg (Ed)., Pseudo-Differential Operators, Roma, C.I.M.E., Cremonese, 1969, pp. 168–305.
[30] J.M. Song, C.C. Lu, W.C. Chew, S.W. Lee, Fast Illinois solver code, IEEE Antennas Propag. Mag. 40 (1998) 27–34.
[31] M.E. Taylor, Pseododifferential Operators, Princeton University Press, Princeton, New Jersey, 1981.
[32] M. Woodworth, A. Yaghjian, Multiwavelength three-dimensional scattering with dual-surface integral equations, J. Opt. Soc. Am. A 11 (4) (1994) 1399–1413.

Please cite this article in press as: O. Bruno et al., Electromagnetic integral equations requiring small numbers of Krylov-subspace iterations, J. Comput. Phys. (2009), doi:10.1016/j.jcp.2009.05.020